

Q^2 evolution of generalized Baldin sum rule for the proton

 Y. Liang,¹ M. E. Christy,² R. Ent,³ and C. E. Keppel^{2,3}
¹Ohio University, Athens, Ohio 45701, USA

²Hampton University, Hampton, Virginia 23668, USA

³Thomas Jefferson National Accelerator Facility, Newport News, Virginia 23606, USA

(Received 26 October 2004; published 15 June 2006)

The generalized Baldin sum rule for virtual photon scattering, the unpolarized analogy of the generalized Gerasimov-Drell-Hearn integral provides an important way to investigate the transition between perturbative QCD and hadronic descriptions of nucleon structure. This sum rule requires integration of the nucleon structure function F_1 , which until recently had not been measured at low Q^2 and large x , i.e., in the nucleon resonance region. This work uses new data from inclusive electron-proton scattering in the resonance region obtained at Jefferson Lab, in combination with SLAC deep inelastic scattering data, to present first precision measurements of the generalized Baldin integral for the proton in the Q^2 range of 0.3 to 4.0 GeV².

 DOI: [10.1103/PhysRevC.73.065201](https://doi.org/10.1103/PhysRevC.73.065201)

PACS number(s): 11.55.Hx, 14.20.Dh, 12.38.Qk, 25.30.-c

I. INTRODUCTION

Polarizabilities are the fundamental quantities that characterize the response of a composite system to static or slowly-varying external electromagnetic fields. The Baldin sum rule connects the sum of the electric and magnetic polarizabilities of the nucleon ($\alpha + \beta$) to the integral of the ν^2 -weighted nucleon unpolarized photoabsorption cross section [1,2],

$$\alpha + \beta = \frac{1}{4\pi^2} \int_{\nu_0}^{\infty} \frac{\sigma_{\frac{1}{2}} + \sigma_{\frac{3}{2}}}{\nu^2} d\nu. \quad (1)$$

Here, $\sigma_{\frac{1}{2}}$ and $\sigma_{\frac{3}{2}}$ are the photoabsorption cross sections of 1/2 and 3/2 helicity states, respectively; ν is the energy carried by the photon; and ν_0 is the pion photoproduction threshold energy. The polarizabilities α and β are defined in the low energy expansion of the Compton scattering amplitudes. In particular, $\alpha + \beta$ represents the helicity nonflip part of the electromagnetic polarizability. The Baldin sum rule establishes a relation between the static nucleon properties (electric and magnetic polarizabilities) and the dynamic nucleon excitation spectrum, such that these polarizabilities can be extracted from precision measurements of the photoabsorption cross sections in real Compton scattering. For the proton, recent measurements give $(\alpha + \beta)_p = 13.69 \pm 0.14$ [3].

The Baldin sum rule is the unpolarized analog of the Gerasimov-Drell-Hearn (GDH) sum rule [4,5] and, in analogy to the generalized GDH sum rule [6], Drechsel, Pasquini, and Vanderhaeghen have used dispersion relation formalism [7,8] to extend the Baldin sum rule to virtual Compton scattering ($Q^2 > 0$, where Q^2 is the square of four-momentum transfer) [9]. We present here first precision measurements of this extended Baldin sum rule for the proton in the Q^2 range of 0.3 to 4.0 GeV².

Extending the GDH and Baldin sum rules to virtual Compton scattering provides a tool to extract generalized polarizabilities by means of radiative electron scattering. These generalized polarizabilities are functions of the Q^2 of the incident photon and describe, in some sense, the spatial distribution of the polarizabilities. After a proof of principle at SLAC [10], the first unpolarized virtual Compton

scattering observables have been obtained from MAMI at $Q^2 = 0.33$ GeV² [11], and recently at Jefferson Lab at higher Q^2 ($1 < Q^2 < 2$ GeV²) [12,13].

The virtual Compton scattering process includes the absorption of the virtual photon, which is related to inclusive electron-nucleon scattering. At finite Q^2 , the generalized sum rule gives

$$\begin{aligned} \alpha(Q^2) + \beta(Q^2) &= \frac{1}{4\pi^2} \int_{\nu_0}^{\infty} \frac{K}{\nu} \frac{\sigma_{\frac{1}{2}} + \sigma_{\frac{3}{2}}}{\nu^2} d\nu \\ &= \frac{e^2 M}{\pi Q^4} \int_0^{x_0} 2x F_1(x, Q^2) dx, \end{aligned} \quad (2)$$

where the integral on the right hand side is the second Cornwall-Norton moment [14] of the nucleon structure function F_1 , barring the elastic contribution. Here, M is the nucleon mass. According to Hand's definition [15], $K = (W^2 - M^2)/2M$ is the equivalent real photon energy needed to excite the nucleon to mass W . The Bjorken scaling variable is $x = Q^2/2M\nu$, and x_0 corresponds to pion threshold.

In the limit of large Q^2 , the coupling constant of quantum chromodynamics (QCD) is very small, and perturbative QCD provides an excellent interpretation of the deep inelastic scattering (DIS) process of electron-proton scattering. In the DIS region, the nucleon structure functions F_L (purely longitudinal), F_1 (purely transverse), and F_2 are related by

$$2xF_1 = \left(1 + \frac{4M^2x^2}{Q^2}\right)F_2 - F_L. \quad (3)$$

On the limit of high Q^2 , $2xF_1 \leq F_2$, and the second moment of the structure function F_1 is less than the first moment of the structure function F_2 which is nearly a constant above $Q^2 = 2$ GeV² [16–19]. Therefore, the integrand in Eq. (2) is less than a constant, and the generalized sum rule ($\alpha + \beta$) will go to 0 as Q^2 goes to ∞ .

At the larger distance scales probed at low Q^2 , the coupling constant of QCD is large, and the scattering process is better described in terms of hadronic degrees of freedom using Chiral Perturbation Theory. The generalized sum rule, then, tends to the Baldin sum rule of real Compton scattering at $Q^2 = 0$.

Between these two regions, a rigorously descriptive theory is lacking at present. Here, the sum rule is dominated by the resonance region structure function. Measuring the generalized Baldin sum rule in this transition region (Q^2 up to a few GeV^2) provides an important window to understand the transition from DIS incoherent processes to the resonance-dominated coherent processes. In practice, we measure the second moment of F_1 in the inclusive electroproduction process, and then extract the generalized Baldin sum rule.

II. EXPERIMENT OVERVIEW

To calculate the integral, F_1 needs to be extracted from the measured cross sections in both the resonance and DIS regions. This requires accurate knowledge of the separated structure function R in both regions, where $R = \sigma_L/\sigma_T$ is the ratio of longitudinal to transverse cross sections. In contrast to the high quality R measurements available in the DIS regime, there were very few R measurements in the resonance region prior to Jefferson Lab experiment E94–110 [20]. Therefore, no precise inclusive F_1 data in the resonance region were available either to constrain the resonance analysis (such as the MAID analysis [21], etc.) or to accurately compute the low Q^2 generalized Baldin sum rule.

E94–110 measured inclusive scattering of unpolarized electrons from a hydrogen target in Hall C at Jefferson Lab (JLab) [20]. The data were accumulated in the nucleon resonance region [20,22], as well as the elastic region with absolute normalizations to better than 2% [23]. The kinematic settings of this experiment were chosen to extract the nucleon structure function R using the Rosenbluth technique at $M^2 \leq W^2 \leq 4 \text{ GeV}^2$. The Q^2 range covered by our data set was between 0.3 and 5 GeV^2 . A complete description of the data analysis and systematic uncertainty estimations may be found in Refs. [20,22,23]. The longitudinal-transverse separations allowed the nucleon structure functions F_2 , F_1 (purely transverse), and F_L (purely longitudinal) to be extracted independently. Formally,

$$R = \frac{F_L}{2xF_1} = \frac{F_2}{2xF_1} \left(1 + \frac{4M^2x^2}{Q^2} \right) - 1. \quad (4)$$

III. ANALYSIS AND RESULTS

A sample of the extracted $2xF_1$ data ($2xF_1 \sim \sigma_T$) in the nucleon resonance and DIS regions is shown in Fig. 1, as a function of Bjorken x at four different Q^2 values. The open triangles in the figure represent the data extracted from the E94–110 Rosenbluth separations, and the open crosses are the data extracted from SLAC Rosenbluth data [24]. The low x NMC data ($0.0045 \leq x \leq 0.25$) are also shown in open circles, which are calculated from the NMC R and F_2 results [25]. While $2xF_1 = 0$ at $x = 0$, NMC results show that $2xF_1 > 0.18$ at $x = 0.0045$ and $Q^2 \geq 0.75 \text{ GeV}^2$. A significant drop-off of $2xF_1$ should take place at $x < 0.0045$. The solid curve was calculated using the R and F_2 parametrization of E94–110 [22] at $W^2 < 4 \text{ GeV}^2$, and using the parametrization of R and F_2 from SLAC DIS experiments [24,26] at $W^2 > 4 \text{ GeV}^2$. Note that the solid curve well reproduces the data in both the

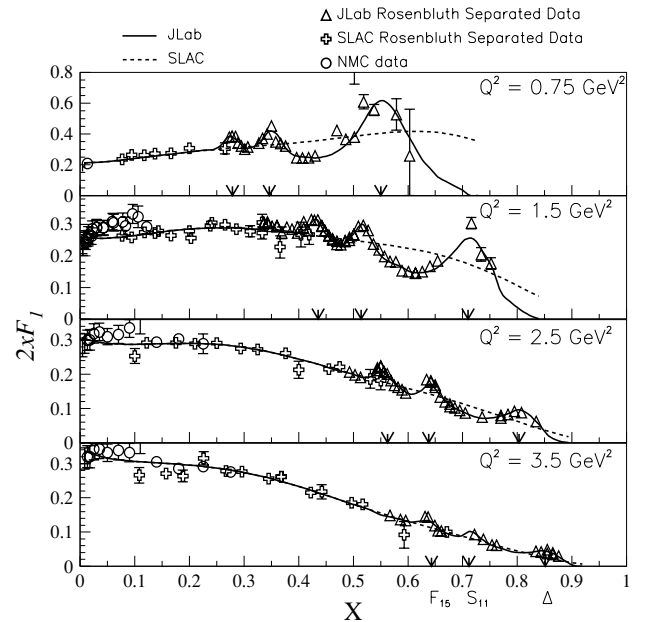


FIG. 1. $2xF_1$ is plotted as a function of Bjorken x , at four different Q^2 values. The three arrows indicate where the three primary resonance enhancements are located.

resonance and DIS regions. The dashed curve in the figure was calculated using only the parametrization of R and F_2 from SLAC DIS experiments [24,26]. A comparison between the JLab E94–110 and SLAC data sets was done at $3.5 < W^2 < 4 \text{ GeV}^2$, and the two data sets were found to be consistent within 1% in this overlap region [22].

As shown in Fig. 1, we calculate the second moment of F_1 by integrating the area below the solid curve over the Bjorken x range $0 < x < x_0$. The area corresponding to $W^2 < 4 \text{ GeV}^2$ represents the resonance contribution to the moment and is calculated using the R and F_2 parametrization of E94–110 [22]; While the area corresponding to $W^2 > 4 \text{ GeV}^2$ is the DIS contribution, and calculated using SLAC parametrization of R and F_2 [24]. The region below $x \sim 0.1$ is extrapolated using the same SLAC parameterization, and the uncertainty associated with this low x extrapolation is less than 1.8% for Q^2 up to a few GeV^2 .

Using this approach, we separated the generalized Baldin sum rule into two pieces, contributions from the resonance and DIS regimes,

$$\alpha(Q^2) + \beta(Q^2) = \frac{e^2 M}{\pi Q^4} \int_{x_{\text{res}}}^{x_0} 2xF_1(x, Q^2) dx + \frac{e^2 M}{\pi Q^4} \int_0^{x_{\text{res}}} 2xF_1(x, Q^2) dx, \quad (5)$$

where x_{res} corresponds to $W^2 = 4 \text{ GeV}^2$. The uncertainty of this extracted generalized sum rule is less than 3.4%, dominated by the normalization systematic uncertainties of the measured cross sections ($\sim 2\%$) [22,24], as well as fitting uncertainties ($\sim 2\%$) [22,24,26] and low x extrapolation uncertainty ($\sim 1.8\%$).

Table I lists the generalized sum rule values at 11 different Q^2 values, as well as the resonance and DIS contributions

TABLE I. Table of the generalized Baldin sum rule values and the associated uncertainty, as well as the resonance and DIS contributions to the sum rule, for the Q^2 values given.

Q^2 (GeV ²)	Sum rule (10 ⁻⁴ fm ³)	Error (10 ⁻⁴ fm ³)	Resonance (10 ⁻⁴ fm ³)	DIS (10 ⁻⁴ fm ³)
0.3	3.0673	0.0871	2.7137	0.3536
0.4	2.2444	0.0636	1.9513	0.2931
0.6	1.2033	0.0341	0.9894	0.2139
0.8	0.6945	0.0197	0.5306	0.1639
1.0	0.4367	0.0124	0.3053	0.1314
1.5	0.1813	0.0051	0.0979	0.0834
2.0	0.0972	0.0028	0.0399	0.0573
2.5	0.0604	0.0017	0.0188	0.0416
3.0	0.0412	0.0011	0.0099	0.0313
3.5	0.0299	0.0009	0.0055	0.0243
4.0	0.0226	0.0006	0.0032	0.0194

separately. Note that the generalized Baldin sum rule extracted from this experiment is not the same as the sum rule extracted from virtual Compton scattering [13]. While these two quantities should converge at $Q^2 = 0$, the measured process of this experiment involves two virtual photons, as compared to one virtual photon in virtual Compton scattering. The latter $\alpha + \beta$ value is 1.51 ± 0.25 (10⁻⁴ fm³) at $Q^2 = 0.92$ GeV² [13], whereas this result is 0.4367 ± 0.0124 (10⁻⁴ fm³) at $Q^2 = 1.0$ GeV².

The extracted extended sum rule value is plotted as a function of Q^2 in Fig. 2, along with the Baldin sum rule at $Q^2 = 0$. It clearly shows that, unlike the generalized GDH sum rule, the generalized Baldin integral evolves smoothly to the $Q^2 = 0$ point as has been predicted [9]. We also plot two MAID estimates, one for the π channel only, and another for the $\pi + \eta + \pi\pi$ channels [27,28], as a comparison to our measurement. The latter agrees better with our data, clearly

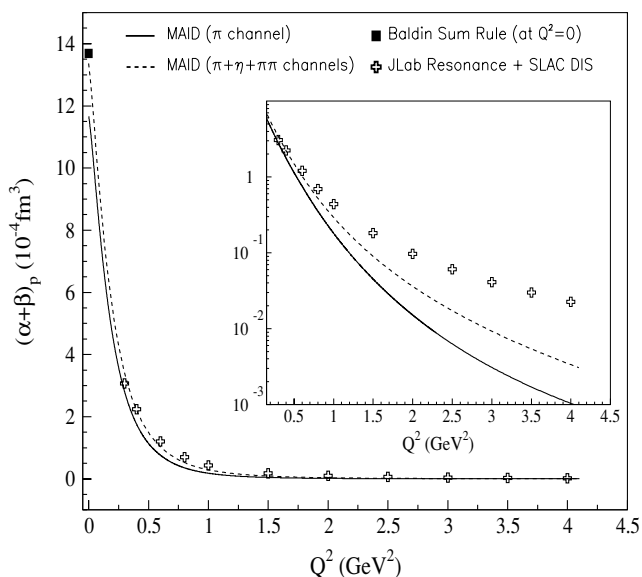


FIG. 2. A comparison of MAID estimates with the extracted sum rule value at different Q^2 .

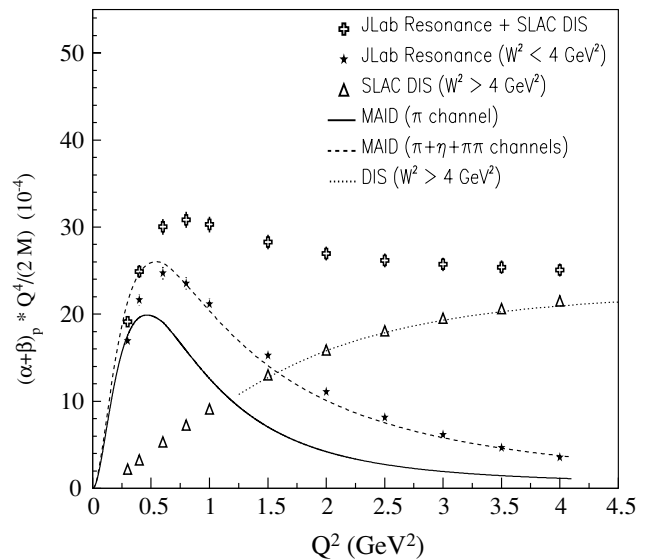


FIG. 3. A comparison of MAID estimates with the generalized Baldin integral weighted by a factor of $Q^4/2M$, at different Q^2 , as well as the resonance and DIS contributions.

indicating that accurate modeling of this integral requires multiple resonance contributions. The discrepancy between the data and MAID estimate at $Q^2 > 1$ GeV² (see figure inset) is likely due to DIS and higher mass contributions of the extracted integral.

To compare the Q^2 evolution of the resonance and DIS contributions of the generalized Baldin integral, we plot the sum rule value, resonance and DIS contributions in Fig. 3, each multiplied by a factor of $Q^4/2M$, as a function of Q^2 , along with the two MAID estimates, and one DIS estimate calculated from the SLAC parametrization [24,26]. The figure shows that the resonance contribution extracted from our data set agrees well with the three channel MAID estimate down to $Q^2 = 0.6$ GeV².

The generalized sum rule is mainly saturated by the resonance contribution at $Q^2 \leq 1$ GeV², while the DIS part dominates at $Q^2 \geq 2$ GeV². At $1 < Q^2 < 2$ GeV², a transition from partonic incoherent processes to resonance dominated coherent processes occurs. Also, the value of $Q^4(\alpha + \beta)/2M$, which is proportional to the second moment of structure function F_1 , is nearly flat at $Q^2 > 2$ GeV². This behavior is predicted by the perturbative description of DIS processes at large Q^2 [16,17].

IV. CONCLUSION

In summary, we have utilized new inclusive electron-proton scattering cross section results in the resonance region, allowing for extraction of the structure functions R , F_2 , F_L , and F_1 . The F_1 data were used to calculate the generalized Baldin sum rule over the Q^2 range from 0.3 to 4.0 GeV². A transition from partonic incoherent processes to resonance dominated coherent processes is observed at Q^2 between 1 and 2 GeV². Resonance models of this integral need to include higher mass contribution. The generalized Baldin sum rule is found to evolve smoothly with Q^2 to the real photon point.

ACKNOWLEDGMENTS

The authors would like to thank Charles Hyde-Wright for many useful discussions. This work was supported in part by research grants 0244999, 0099540, and 9633750 from the

National Science Foundation. The Southeastern Universities Research Association operates the Thomas Jefferson National Accelerator Facility under U.S. Department of Energy contract DEAC05-84ER40150.

-
- [1] A. M. Baldin, Nucl. Phys. **18**, 310 (1960).
 [2] L. I. Lapidus, Sov. Phys. JETP **16**, 964 (1963).
 [3] D. Babusci, G. Giordano, and G. Matone, Phys. Rev. C **57**, 291 (1998).
 [4] S. B. Gerasimov, Sov. J. Nucl. Phys. **2**, 430 (1966).
 [5] S. D. Drell and A. C. Hearn, Phys. Rev. Lett. **16**, 908 (1966).
 [6] M. Anselmino, B. L. Ioffe, and E. Leader, Sov. J. Nucl. Phys. **49**, 136 (1989).
 [7] R. de L. Kronig, J. Opt. Soc. Amer. Rev. Sci Instrum. **12**, 547 (1926); H. A. Kramers, Atti Congr. Int. Fis. Como. **2**, 545 (1927).
 [8] F. E. Low, Phys. Rev. **96**, 1428 (1954).
 [9] D. Drechsel, B. Pasquini, and M. Vanderhaeghen, Phys. Rep. **378**, 99 (2003).
 [10] J. F. J. vandenBrand *et al.*, Phys. Rev. D **52**, 4868 (1995).
 [11] J. Roche *et al.*, Phys. Rev. Lett. **85**, 708 (2000).
 [12] S. Jaminion *et al.*, hep-ph/0312293, submitted to Phys. Rev. Lett. (2004).
 [13] G. Laveissiere *et al.*, hep-ph/0312294, submitted to Phys. Rev. Lett. (2004).
 [14] J. M. Cornwall and R. E. Norton, Phys. Rev. **177**, 2584 (1969).
 [15] L. N. Hand, Phys. Rev. **129**, 1834 (1963) (1968).
 [16] A. De Rujula, H. Georgi, and H. D. Politzer, Ann. Phys. (NY) **103**, 315 (1977).
 [17] A. De Rujula, H. Georgi, and H. D. Politzer, Phys. Lett. **B64**, 428 (1977).
 [18] C. S. Armstrong R. Ent, C. E. Keppel, S. Liuti, G. Niculescu, and I. Niculescu, Phys. Rev. D **63**, 094008 (2001).
 [19] W. Melnitchouk, R. Ent, and C. E. Keppel, Phys. Rep. **406**, 127 (2005).
 [20] Y. Liang *et al.*, nucl-ex/0410027, submitted to Phys. Rev. Lett. (2004).
 [21] T. Mart *et al.*, <http://www.kph.uni-mainz.de/MAID/>
 [22] Y. Liang, Ph.D. thesis, The American University, 2003.
 [23] M. E. Christy *et al.*, Phys. Rev. C **70**, 015206 (2004).
 [24] L. W. Whitlow *et al.*, Phys. Lett. **B250**, 193 (1990).
 [25] Arneodo *et al.* Nucl. Phys. **B483**, 3 (1997).
 [26] K. Abe *et al.*, Phys. Lett. **B452**, 194 (1999).
 [27] D. Drechsel *et al.*, Nucl. Phys. **A645**, 145 (1999).
 [28] D. Drechsel, S. S. Kamalov, and L. Tiator, Phys. Rev. D **63**, 114010 (2001).